

First-Principles and Quantum Transport Studies of Metal-Graphene End Contacts

Cheng Gong,¹ Geunsik Lee,¹ Weichao Wang,¹ Bin Shan,¹ Eric M. Vogel,^{1,2}
Robert M. Wallace,^{1,2} and Kyeongjae Cho^{1,3,*}

¹Department of Materials Science & Engineering, ²Department of Electrical Engineering, and ³Department of Physics, The University of Texas at Dallas,
Richardson, Texas, 75080, USA

*Corresponding author: kjcho@utdallas.edu

ABSTRACT

Metal-graphene contact is of critical significance in graphene-based nanoelectronics. There are two possible metal-graphene contact geometries: side-contact and end-contact. In this paper, we apply first-principles calculations to study metal-graphene end-contact for these three commonly used electrode metals (Ni, Pd and Ti) and find that they have distinctive stable end-contact geometries with graphene. Transport properties of these metal-graphene-metal (M-G-M) end-contact structures are investigated by density functional theory non-equilibrium Green's function (DFT-NEGF) algorithm. The Transmission as a function of chemical potential ($E-E_F$) shows asymmetric curves relative to the Fermi level. Transmission curves of Ni-G-Ni and Ti-G-Ti contact structures indicate that bulk graphene sheet is n-doped by Ni and Ti electrodes, but that of Pd-G-Pd shows p-doping of graphene by Pd electrode. The contact behaviors of these electrodes are consistent with experimental observations.

INTRODUCTION

Graphene is a promising channel material candidate to continue the device scaling in post-silicon CMOS regime. Metal-graphene contact is a crucial structure in the overall performance of graphene-based devices: not only the total device resistance mainly originates from contact resistance,¹ but also metal electrodes can significantly modify graphene's intrinsic properties and endow graphene-based devices with many novel properties and performances.^{2,3,4} Symmetry^{5,6,7} between electron and hole conduction in graphene devices has attracted lots of recent research efforts as it reflects the unique electronic structure of graphene.

There are two different types of contact geometries between metal electrode and graphene sheet: side-contact (metal surface parallel to graphene basal plane) and end-contact (metal surface perpendicular to graphene basal plane). However, nearly all relevant research works are exclusively focused on side-contact geometry. In spite of much investigation, there is still no close agreement between theoretical and

experimental studies on the nature of metal-graphene contacts. In the simulation works, most efforts are focusing on weakly-interactive metals^{2,7} which preserve graphene's intrinsic π -band structure with observable doping effect. However, experimental studies have shown a preference for strongly-interactive metals such as Ni, Pd, Ti and Cr which can stick to graphene coherently and form mechanically stable contacts for realistic device fabrication.^{5,8} Considering these differences, there is a need to study metal-graphene contact for strongly interacting metal species to examine the consistency between theoretical and experimental studies.

From a practical point of view, experimentalists conventionally deposit metal electrode on a graphene placed on an insulating substrate (e.g., SiO₂) rather than placing graphene sheet on prefabricated metal electrodes. The metal electrode deposition process is chemically reactive, and it is reasonable to expect that the metal electrodes may dissolve carbon atoms and destroy the graphene underneath the deposited metal. Such metal deposition process would result in an end-contact structure between the edge of the metal electrode and the remaining intact graphene sheet (see Fig. 1a). It is worthwhile to note that a similar metal contact issues have been raised for carbon nanotube electronics, and it has been suggested that the charge injection at the metal-nanotube interface is happening at the edge of the contact electrodes. Due to the absence of theoretical understanding on the metal-graphene end-contact, a theoretical investigation can provide much needed insight and understanding on the electronic structures and charge injection characteristics at the end-contacts.

We apply first-principles calculations to Ni-, Pd-, and Ti-G end-contact structures. Stable contact geometries are identified as the lowest energy structures from interface geometry optimization in which the standing graphene sheets are shifted on metal surfaces along x-, y- and xy-directions (as shown in Fig. 2d). Based on the obtained stable contact geometries, non-equilibrium Green's function (NEGF) algorithm based on density functional theory (DFT) program SIESTA is used to investigate the transport properties of Ni-G-Ni and Pd-G-Pd end-contact structures. Equilibrium Fermi level is readjusted after these contacts are integrated into a device structure. Bulk graphene sheet is doped as a result of the difference between the Dirac point and equilibrium Fermi level of the device system. Consequently, junctions are formed within graphene sheet and induce asymmetry between electron and hole conduction in these M-G-M end-contact device structures.

METHODOLOGY

The initial DFT calculations to search the most stable contact geometry are performed in Vienna *Ab initio* Simulation Package (VASP)⁹ with the projected augmented wave pseudopotentials with local density approximation. Energy cutoff of 400 eV is chosen for the plane-wave basis which shows a good convergence in total energy and Hellman-Feynman forces. Metal surfaces' lattice sizes are strained to fit graphene's periodic length 2.46 Å along zigzag edge. Graphene is standing perpendicular to

metal surfaces with zigzag edge attached to metal as shown in Fig. 1. To optimize the interface geometry, graphene sheets are shifted on top of metal surfaces along three high symmetric lines: two lattice vectors and a diagonal of the unit cell (shown in Fig. 2). For each shift, metal lattices are fixed and graphene's z-coordinates perpendicular to metal surfaces are relaxed. Most stable contact geometries are found by the total energy comparison between these sampling structures. For this DFT calculation, hydrogen atoms are used to passivate the edge of sixth hexagon away from interface to mimic the bulk C-C bond in graphene. Spin polarized calculation is performed only in Ni electrode systems. Based on the stable contact geometries, full M-G-M device structures are set up for DFT (SIEAST)-NEGF calculations^{10,11}. In this part of first-principles calculations, we used numerical atomic type orbital basis sets and Troullier-Martin type pseudopotentials¹². The single-zeta basis set was used for the electronic density matrix and transmission values calculations. Cutoff energy of 150 Ry for the grid mesh is chosen. The technical details of the non-equilibrium Green's function method are given in Ref. 10. Contour integration on the imaginary plane was used to obtain the density matrix from the Green's function. We used 33 contour points, with the lowest energy bound of 2.5 Ry in the contour diagram for the zero bias case.

Results and Discussions

Metal's FCC (111) surface and HCP (0001) surface can be mapped onto graphene's lattice with ease for side-contact.³ Similarly, graphene sheet can stand perpendicular to metal surface with zigzag edge contacting metal. The intrinsic lattice mismatch is reasonably small (Ni 1.2% compressed, Pd 3.2% stretched, and Ti 3.7% compressed) so that metal lattice can be strained a little to match the lattice constant of graphene. In addition, periodic boundary condition is applied in the calculations

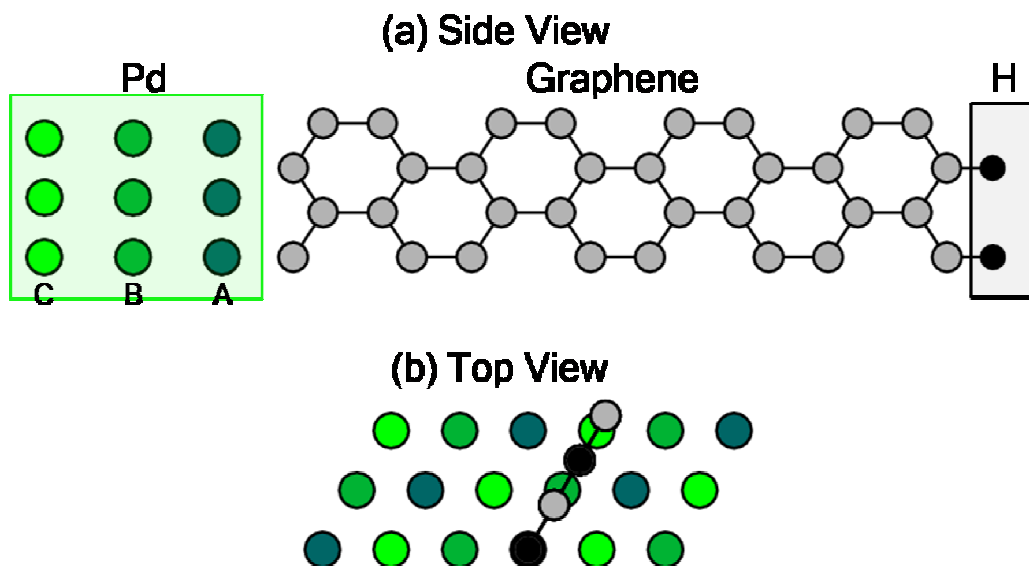


Figure 1. (a) Side view of Pd-G end-contact structure; (b) Top view of Pd-G end-contact structure. Periodic boundary condition is applied along graphene's zigzag edge direction.

Figure 1 (a) and (b) show the side and top views of graphene standing on top of Pd FCC (111) surface. Initially, the position 0 (notated in Fig. 2b) represents the position of carbon atom in the unit cell exactly on top of a surface Pd atom, and the other carbon atom at the interface is on top of the bridge center of the lattice vector. Graphene sheets are shifted along three high symmetry directions by different lengths based on the different repetitive periodic lengths. Along each direction, 7 shifting steps are sampled. Total energy calculations show that the most stable structures are graphene carbon atoms sitting on the hollow site of Ni lattice, on the top site of Pd lattice, and on the bridge center site of Ti lattice, respectively (as shown in Fig. 2 (a), (b), and (c)). The equilibrium interface distance between bottom carbon atoms and metal surface planes are 1.55 Å (Ni), 1.72 Å (Pd), and 1.58 Å (Ti).

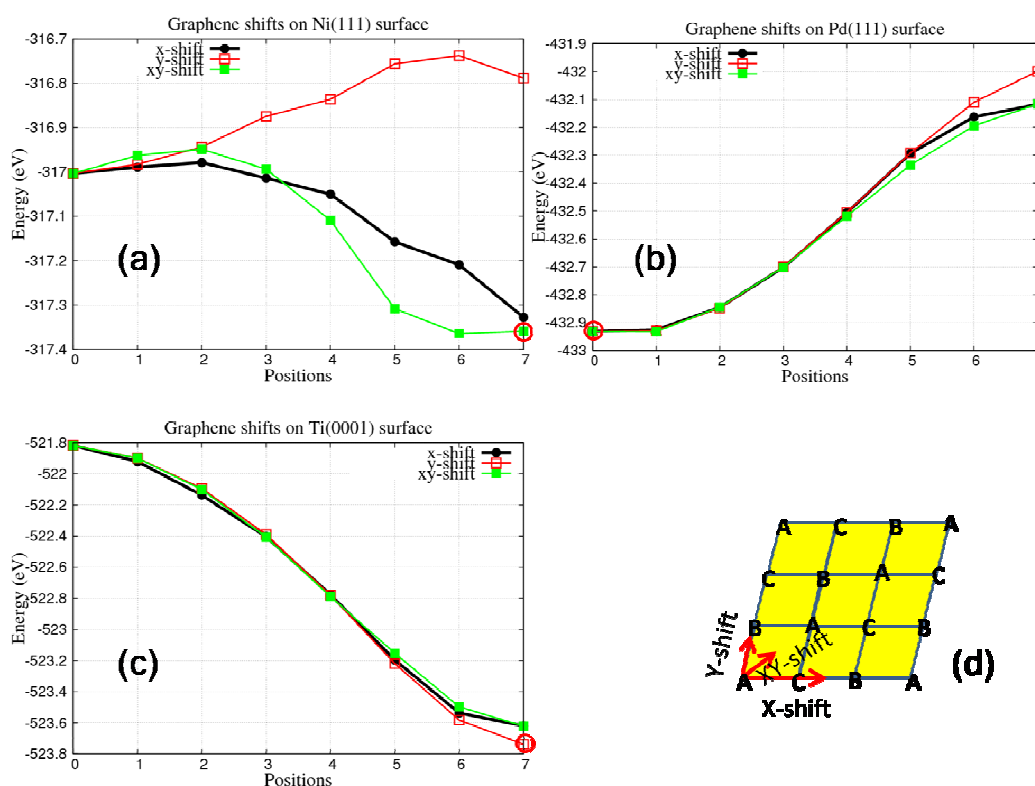


Figure 2. Total energy of grapheme-metal interface as grapheme sheet is shifted on the metal ((a) Ni, (b) Pd, and (c) Ti) surfaces. Three high symmetry directions along which grapheme is shifted are indicated in (d).

Based on the different stable end-contact geometries between graphene and Ni, Pd, and Ti, we set up the whole device structures with two end contacts as illustrated in Fig. 3. Shaded rectangular zones represent left and right leads, and scattering region (interface) and channel part (graphene) are arranged between left and right leads.

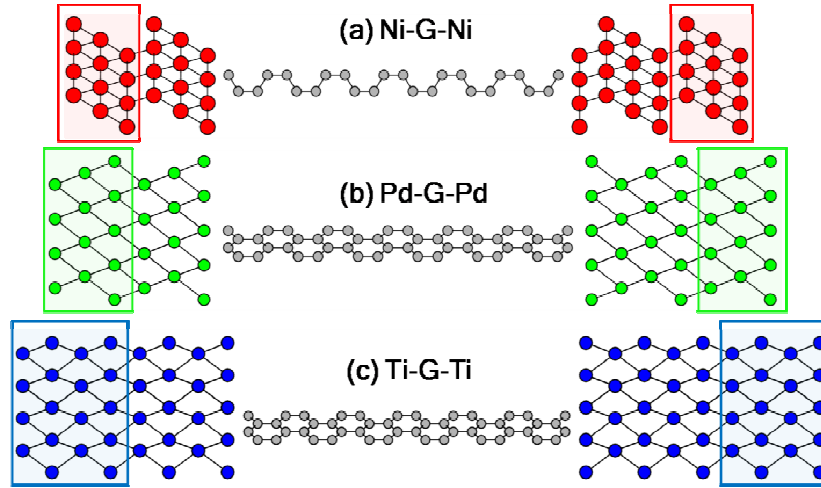


Figure 3. Ni-G-Ni, Pd-G-Pd, and Ti-G-Ti end-contact device structures. Periodic boundary conditions are applied along graphene's zigzag edge directions.

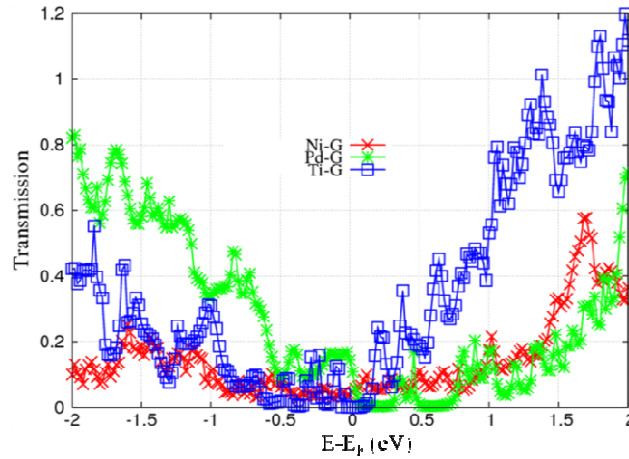


Figure 4. Transmission curves of Ni-G-Ni, Pd-G-Pd and Ti-G-Ti end-contact devices.

Transport studies show that the transmission curves as a function of Fermi level (representing gate voltage change) these device structures are asymmetric (Fig. 4), indicating the asymmetry between electron and hole conduction. This asymmetric transmission characteristic originates from carriers' different transmissions through graphene p-p junction, n-n junction and p-n junctions.¹³ Fig. 4 indicates that bulk graphene is n-doped by Ni and Ti end-contacts, and p-doped by Pd end-contact. When bulk graphene is n-doped by Ni and Ti electrodes, n-n-n junction and p-n-p junction will be formed by adjusting gate voltage to positive values and negative values. Since p-n-p junction blocks carriers' transmission more than n-n-n junction, in Ni-G-Ni end-contact structure, electron conduction is larger than hole conduction. For Pd-G-Pd end-contact structure, p-doped graphene forms n-p-n and p-p-p junctions under positive and negative gate voltage leading to larger hole conduction under negative gate voltage. These findings are consistent with the experimental data indicating that the end-contact structure may have formed in the experimentally studied graphene device structures.

Conclusion

DFT optimization of the interface geometry shows that Ni, Pd, and Ti have different stable end-contact geometries. Full M-G-M device structures are prepared from the optimized stable contact geometries. DFT (SIESTA)-NEGF algorithm is applied to investigate the transport properties of the M-G-M device structures. The resulting transmission shows that due to the doping of bulk graphene by metal electrodes, junctions are formed in the channel part. Junction-induced asymmetric transmission between electrons and holes are observed by quantum transport calculation.

Acknowledgements

The work is funded by SWAN (Southwest Academy of Nanotechnology) and Lockheed Martin Inc. Calculations are done on TACC (Texas Advanced Computer Center) and MSL (Multiscale Simulation Lab cluster at UT Dallas). The authors would like to thank the SWAN team members for insightful discussions during weekly graphene meetings at UT Dallas.

References

-
- ¹ A. Venugopal, L. Colombo, and E. M. Vogel, *Appl. Phys. Lett.* **96**, 013512 (2010)
 - ² G. Giovannetti, P. A. Khomyakov, G. Brocks, V. M. Karpan, J. van den Brink, and P. J. Kelly, *Phys. Rev. Lett.* **101**, 026803 (2008).
 - ³ C. Gong, G. Lee, B. Shan, E. M. Vogel, R. M. Wallace, and K. Cho, *Phys. Rev. B* (submitted)
 - ⁴ E. J. H. Lee, K. Balasubramanian, R. T. Weitz, M. Burghard, and K. Kern, *Nature Nanotech.* **3**, 486 (2008)
 - ⁵ B. Huard, N. Stander, J. A. Sulpizio, and D. Goldhaber-Gordon, *Phys. Rev. B* **78**, 121402 (R) (2008).
 - ⁶ K. Pi, K. M. McCreary, W. Bao, Wei Han, Y. F. Chiang, Y. Li, S.-W. Tsai, C. N. Lau, and R. K. Kawakami, *Phys. Rev. B* **80**, 075406 (2009)
 - ⁷ S. B.-Lopez, M. Vanevic, M. Kindermann, and M.Y. Chou, *Phys. Rev. Lett.* **104**, 076807 (2010)
 - ⁸ X. Wang, Y. Ouyang, X. Li, H. Wang, J. Guo, and H. Dai, *Phys. Rev. Lett.* **100**, 206803 (2008)
 - ⁹ G. Kresse, and J. Furthemüller, *Comput. Mater. Sci.* **6**, 15 (1996)
 - ¹⁰ W. Y. Kim, K. S. Kim, *J. Comp. Chem.* **29** 1073 (2008)
 - ¹¹ W. Y. Kim, K. S. Kim, *Nature Nantech.* **3** 408 (2008)
 - ¹² J. M. Soler, E. Artacho, J. D. Gale, A. García, J. Junquera, P. Ordejón, and D. S.-Portal, *J. Phys. Condens. Matter* **14**, 2745–2779 (2002)
 - ¹³ T. Low, S. Hong, J. Appenzeller, S. Datta, and M. Lundstrom, *IEEE TRANSACTIONS ON ELECTRON DEVICES*, VOL. **56**, NO. 6 (2009)